Hindawi
Advances in Civil Engineering
Volume 2019, Article ID 6519189, 16 pages
https://doi.org/10.1155/2019/6519189

Research Article

Large-Deformation Failure Mechanism of Coal-Feeder Chamber and Construction of Wall-Mounted Coal Bunker in Underground Coal Mine with Soft, Swelling Floor Rocks

Xingkai Wang,[1,2] Wenbing Xie ,[1] Jianbiao Bai,[1] Shengguo Jing,[2] and Zhili Su[2]

[1]*State Key Laboratory of Coal Resources and Safe Mining, China University of Mining and Technology, Xuzhou 221116, China*
[2]*School of Mines, China University of Mining and Technology, Xuzhou 221116, China*

Correspondence should be addressed to Wenbing Xie; 1692@cumt.edu.cn

Received 21 March 2019; Revised 25 June 2019; Accepted 11 July 2019; Published 15 August 2019

Academic Editor: Marco Corradi

In traditional vertical coal bunker systems, a coal-feeder chamber (CFC) must bear the whole weight of the bunker. However, maintenance of CFCs within soft, swelling floor rock is a challenge faced in underground coal mines. Floor-heave control is a complex problem and is still not well-solved. Moreover, there is no report on the construction of bunker without a CFC, especially under such weak floor-rock conditions. Based on the serious CFC collapse case at Xiashijie mine, China, this work analyzed the deformation characteristics, main influencing factors, and failure mechanisms of the CFC using a FLAC numerical model. The results indicate that the intrusion of water weakens the strength of the floor rock and causes significant expansive forces; thus, large deformations and tensile failure occur first in the floor, further causing shearing and tensile damage of the reinforced column and even overall instability of the CFC. Then, a new wall-mounted coal bunker (WMCB), without building the CFC, is proposed. The FLAC3D program was adopted to study the stability of the rocks surrounding the new bunker, and an optimized reinforcement scheme was determined. More importantly, a self-bearing system, which includes self-designed H-steel beams, H-steel brackets, and self-locking anchor cables, was proposed and constructed to bear the whole weight of the bunker. The stability of WMCB was verified by a theoretical safety assessment and field test. The invented WMCB could remain stable in spite of severe floor heave. This work can provide helpful references for the construction of vertical bunkers without CFCs in coal mines with soft, swelling floor rocks.

1. Introduction

Raw coal, produced at the working face in underground coal mines, should be transported to the surface via a transportation system (Figure 1), which commonly includes a coal strap transporting system in the longwall panel entry, coal-storage bunker installed in the mining area, conveyor belt in the main haulage roadway, coal bunker at the bottom of the shaft, and main shaft hoisting system. It is clear that the storage bunker plays an indispensable role in coal transportation. In addition, the use of bunkers can reduce the effect of transportation interruptions and congestion [1, 2], increase mining system availability [3], and improve transportation efficiency [4, 5]. The bunker usually contains a bottom coal bunker, district coal bunker, section coal bunker, ground bunker, and tunnel bunker [4], all of which are generally divided into the three forms: horizontal, vertical, or inclined. Overall, horizontal coal bunkers are used widely in the United Kingdom, the United States, Canada, the former Soviet Union, etc. However, China, one of the largest coal-mining countries, mainly researches and builds vertical coal bunkers [2].

Vertical bunkers have been used widely in China for many years. Figure 2(a) shows the structure of a traditional vertical bunker, which includes the coal bunker body and the coal-feeder chamber (CFC), which is constructed in the belt haulage roadway and bears the whole weight of the coal in the bunker, concrete silo, and coal-feeder machine. The belt conveyors feed into the top of the bunker from either vibrofeeders or variable-speed belt feeders loading out at the bottom [6]. Thus, the stability of the CFC is crucial to ensure the bunker works effectively. Here, coal bunker #214 could not be used owing to the severe collapse that occurred in the CFC even though it was repaired annually, and many effective measures were taken to improve the stability of the

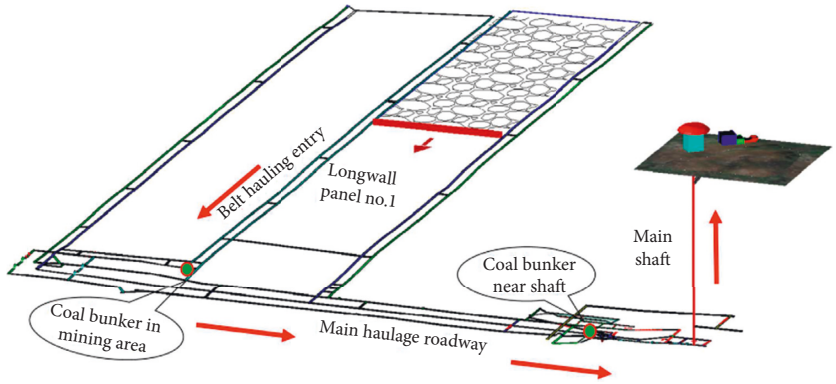

Figure 1: Coal transportation system in an underground coal mine.

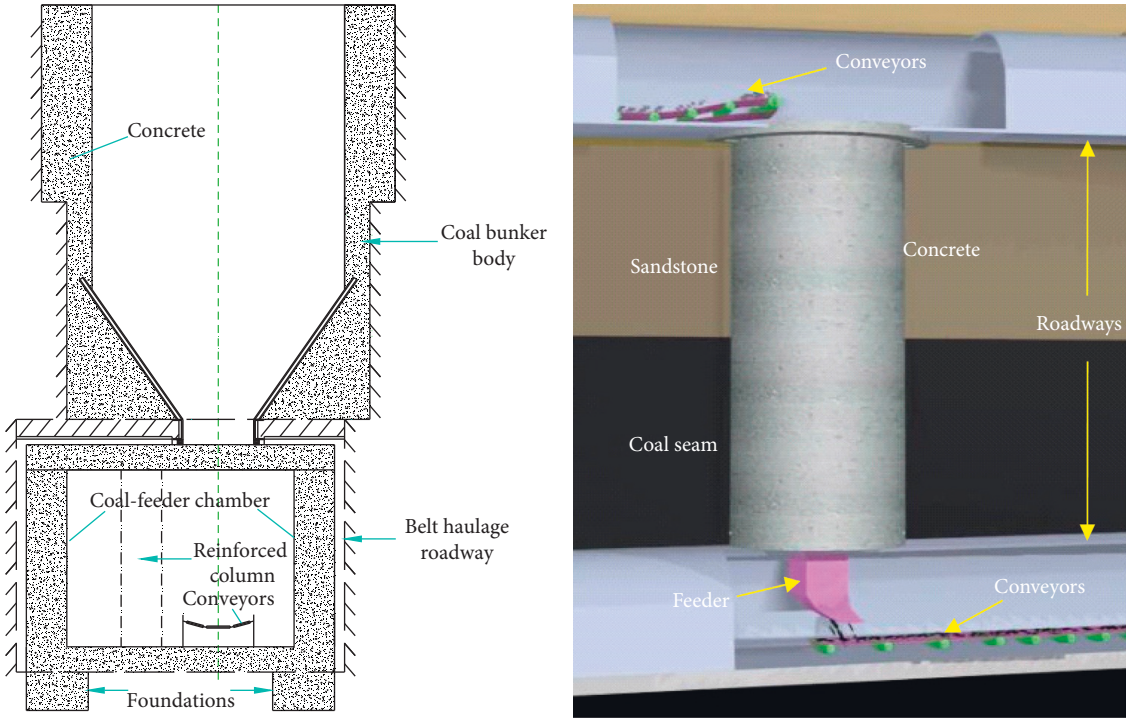

Figure 2: Structure of (a) traditional vertical bunker #214 and (b) the new designed vertical bunker without CFC.

load-bearing structure of the CFC. Figure 3 shows the large deformation that occurred in the CFC.

On the one hand, much research has been devoted to study floor heave of chamber in coal mines [7–10]. Nevertheless, floor-heave control is a complex problem in underground coal mines; the solution approaches are commonly a combination of bolts, anchor cables, concrete, and steel inverted arches, and such construction techniques are not only difficult to carry out in the field but the application effect is also poor. On the other hand, the study of the existing literature for coal bunker mainly focuses on (i) the optimum bunker size and location selection in underground coal mine conveyor systems [3, 11], (ii) the construction of the coal bunker with a large diameter and vertical height [12, 13], (iii) the optimization of methods of safe construction under different geological conditions [14, 15], (iv) the deterioration and collapse mechanism of the reinforced concrete bunker [16], (v) the curing technique of blockage and fractures in the walls of the coal bunker body [17–19], and (vi) the maintenance of the coal bunker [20–22]. Those studies have made significant progress. However, there are no generally accepted cases applicable to construction of a new type of vertical coal bunker (Figure 2(b)) without a CFC, especially when the CFC of the traditional coal bunker could not be stable within weak floor rock.

This work used field surveys, theoretical analysis, laboratory tests, and numerical simulation to analyze the main factors causing floor heave and the failure mechanism of the CFC. Then, a new coal bunker, called a wall-mounted coal bunker (WMCB), without a CFC was invented and

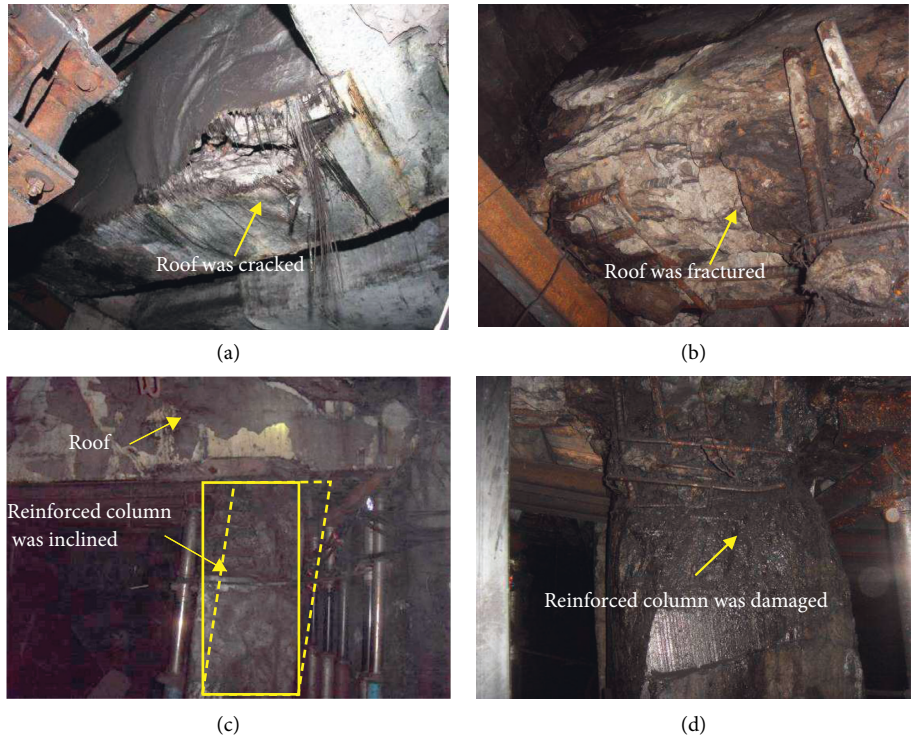

Figure 3: Collapse characteristics of the CFC in coal bunker #214. (a) The roof was cracked. (b) The roof was fractured. (c) The reinforced concrete column was inclined. (d) The reinforced concrete column was damaged.

designed, and its key technological bases were investigated. This work focused on the construction method of a self-bearing system to transfer the entire weight borne by the CFC into the rock surrounding the coal bunker. Finally, the security and the reliability of the new coal bunker were discussed, and it was implemented at Xiashijie coal mine.

2. Background

2.1. Geological Conditions. As shown in Figure 4, coal bunkers #214 and #3 (the new bunker), both vertical bunkers, are located in the belt haulage roadway near the 953 sump in Xiashijie coal mine, Tongchuan Coal Mining Group Co. Ltd. Coal bunker #214 is the original coal-storage bunker, with a height and diameter of 8.7 m and 5 m, respectively. It is noted that coal bunker #214 is located entirely within coal seam #4-2, the two walls of CFC-surrounding rock are also part of coal seam #4-2, and the floor is mudstone. Coal bunker #3 is built to replace coal bunker #214 because of the latter's repeated failures. Coal bunker #3 is 5 m in diameter and 15 m in height, and its upper surrounding rock is coarse sandstone and siltstone, of which the thicknesses are 3.2 m and 5.8 m, respectively. The lower part of the surrounding rock is coal seam #4-2, with a thickness of 6 m.

2.2. CFC Failure Mechanism

2.2.1. Deformation Characteristics of the CFC. The CFC's load-bearing structure is composed of the roof, floor, and side walls, which are made of reinforced concrete. Figure 3 shows the deformation and collapse of the CFC, even though the CFC was repaired twice and was recently reinforced by a concrete column between the walls. The convergence of the chamber was measured by the crossing method [23] after the latest repair. The deformation data collected after monitoring for three months is shown in Figure 5; the roof-floor and wall-wall convergences in the CFC were 1632 mm and 218 mm, respectively. Based on the onsite damage features and the deformation data, the main deformation characteristics could be concluded as follows:

(1) Large deformation of the floor: the cumulative roof-floor convergence was much greater than the convergence of the walls in the CFC, whereas the onsite deformation shows that the roof subsidence was not obvious (less than 150 mm), but severe floor heave occurred

(2) Collapse and failure constantly emerge after repair in the CFC (especially the floor): the load-bearing structure of the CFC could only remain stable for three months after repair; this was mainly attributed to the mudstone and clay materials of the immediate and hard floors, respectively, which are weak and soft in nature and swell severely when water is encountered.

2.2.2. Main Influencing Factors. According to the in situ survey and rock expansion experiments, the main factors inducing failure of the CFC are as follows:

(1) The swelling property of the CFC floor rocks: the swelling properties of the mudstone and clay were

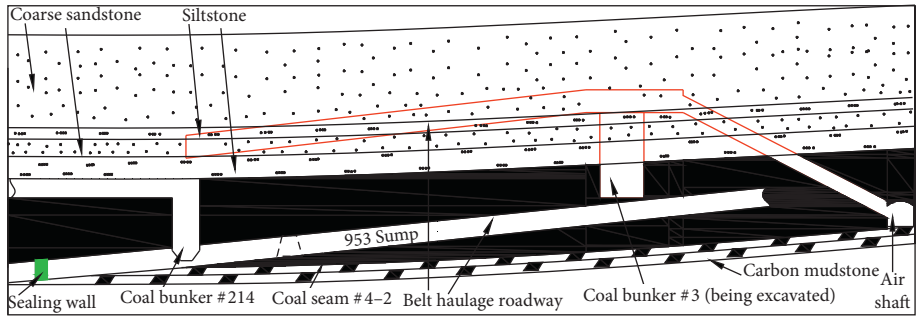

Figure 4: Geological cross section through coal bunkers #214 and #3.

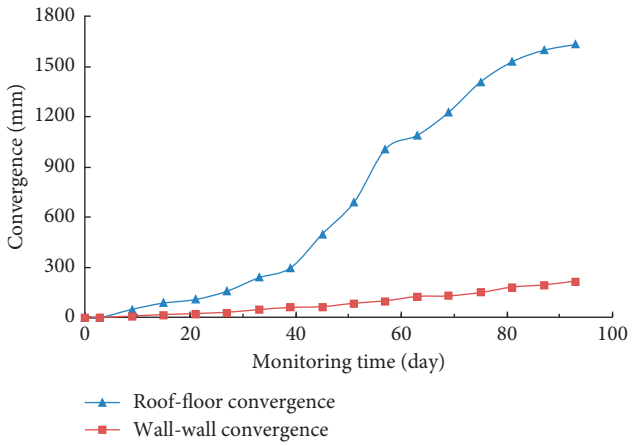

Figure 5: CFC deformation monitoring results.

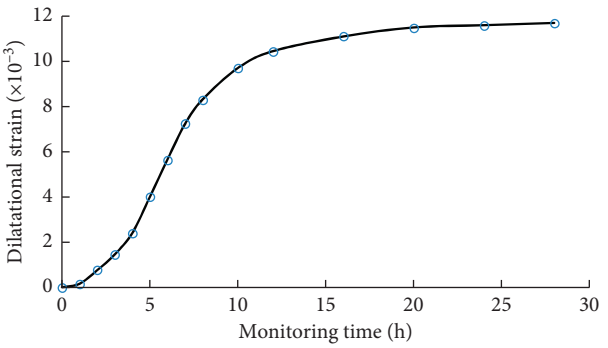

Figure 6: Rock expansion experiment results.

verified by the laboratory tests, i.e., the rock-expansion experiments [24]. Figure 6 shows the dilatational rate of the floor strata mudstone, which increased after immersion in water for 2 h and then reached the maximum of 11700 $\mu\varepsilon$ after 12 h. Mineral-composition analysis by electron microscope found that the mudstone and clay rocks contain abundant minerals, such as kaolinite, montmorillonite, and illite. These minerals contained in the immediate floor and hard floor account for as much as 82% and 85%, respectively, meaning that the floor rocks are liable to swelling, which is not conducive to chamber stability.

(2) The rich supply of mine water under these geological conditions: with a continuous supply of water from the seepage in the working-face goafs, sump #953 above, and the productive water in the belt roadway (Figure 4), the swelling floor rocks would have lower strength and generate a significant expansive force; thus, the concrete walls and floor of the chamber were crushed after repair and reinforcement, further causing the collapse in the chamber roof and inducing instability of the whole bearing structure.

2.2.3. Influence of Water on the Floor Heave and Failure of CFC. Numerical simulation, as a basic method, is widely used to determine the stresses or displacements in underground spaces [25, 26], analyze the failure mechanism or stability of engineering rock masses [13, 27–30], optimize support schemes for roadways [23], simulate experimental tests and verify the results thereof, etc. In this study, the influence mechanism of water on floor heave and overall failure occurring in CFC was investigated by using a FLAC2D model. According to the main research of this work, the simplified model was established, as shown in Figure 7. The boundary conditions were set as follows: a vertical stress of 9.8 MPa was applied on the upper boundary of the numerical model to simulate the overlying strata pressure (burial depth was nearly 400 m); a horizontal stress of 6.5 Mpa was applied to the left and right boundaries, which were fixed in displacement in the normal direction; and the lower boundary was fixed in the vertical direction. Based on the laboratory experiments and the deformation information supplied by the coal mine, the properties of the coal and rock mass were determined by considering the Hoek–Brown failure criterion [31, 32]. Additionally, a strain-softening constitutive model (Figure 8) was selected. For simplicity, the friction angle remained unchanged while the cohesion of the rock mass gradually reduces to its residual value (0.1 MPa), at which the plastic shear strain threshold is 0.3%. The coal and rock physical and mechanical parameters used in this model are shown in Table 1. However, the intrusion of water weakens the mechanical connection between rock and mineral particles, which leads to the decrease of the cohesion of rock mass and the weakening of the physical and mechanical properties of rock mass [34]. Figure 6 shows that the swelling of the rock was not obvious after 30 h; thus, the mechanical parameters of the floor strata that were immersed in water for 36 h were measured by experimental tests, as given in Table 2. During numerical modeling, the

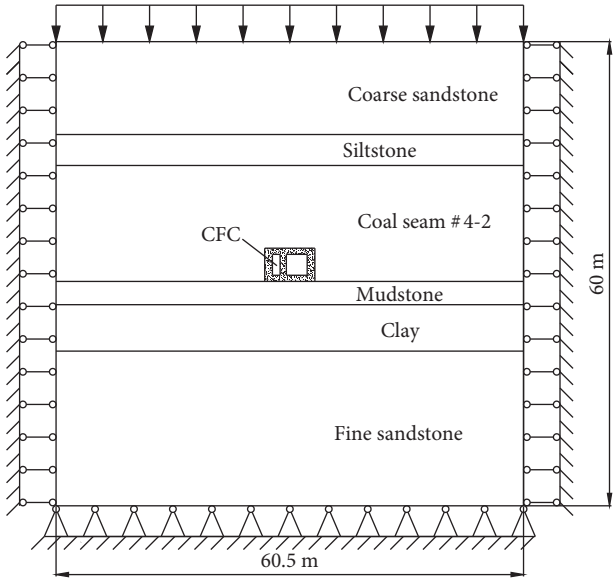

Figure 7: Numerical model.

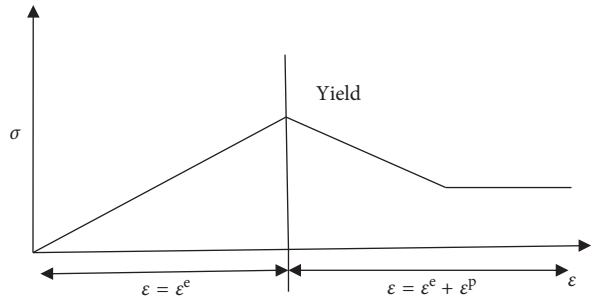

Figure 8: Strain-softening constitutive model [33], where ε^e is the elastic strain and ε^p is the plastic strain.

normal stiffness (k_n) and shear stiffness (k_s) of the interface between the concrete and surrounding rock could be determined by the following equation [33]:

$$k_n = k_s = 10\left[\frac{K + (4/3)G}{\Delta z_{min}}\right], \quad (1)$$

where K and G are the bulk and shear moduli, respectively, and Δz_{min} is the smallest width of an adjoining zone in the normal direction.

To understand the influence of mine water on the failure of the CFC, the distribution of both plastic zones (Figure 9) and displacement (Figure 10) in CFC were simulated under conditions with and without water. Because mine water was encountered, the strength of the floor rocks decreased and swelling rock generated significant expansive forces, and a much larger ranging plastic zone appeared in the rock surrounding the floor and walls in Figure 9(b) (the maximum plastic zone reached 5.8 m in the sides and floor) than that in Figure 9(a) (the maximum plastic zone only reached 2.4 m in the roof). Apparently, tension and shearing damage occurred in the roof (Figure 9(b)), which induced cracking and fracture of the roof (as shown in Figure 3). Moreover, the bottom beam of the CFC was almost completely in a state of tensile failure, and the reinforced column was mainly subject to shearing and tension damage, further causing severe shear dilatancy. The collapse characteristics of the CFC were in line with the field photograph (Figure 3).

In addition, comparison of displacement distributions without and with influence of water (Figure 10) showed the displacement of the chamber affected by mine water (maximum value of 643 mm) was much greater than that without the influence of water (maximum value of 24 mm). More importantly, without the influence of water, the deformation of the surrounding rock was mainly a result of roof subsidence; the floor and reinforced column deformations were small. However, with the influence of water, a large amount deformation appeared in floor and column, while the deformations of the roof and two sides were small, as shown in Figure 10(b), which was in good agreement with in situ monitoring data (Figure 5). In summary, the floor heave, caused mainly by mine water, is the underlying cause of the instability and repeated failure of concrete in CFC.

Even though many measures were taken, such as the drainage of the mine water, installation of U36 steel inverted arches, and reinforcement of the bottom beams, it was still difficult to control the floor heave. Thus, coal bunker #214 could not work properly.

3. Key Techniques of the WMCB

As discussed previously, severe floor heave is the main factor inducing instability of the CFC under this geological condition, and no solution has been proven to be an effective reinforcement method to maintain the traditional coal bunker. It would be better to invent a new type of coal bunker without building the CFC to replace coal bunker #214. Thus, the weight borne by the CFC should be transferred to a newly designed bearing system in the WMCB.

3.1. Reinforcement Scheme of the Rock Surrounding the Coal Bunker. First, the rock surrounding the bunker, in which a variety of load-bearing structures of the coal bunker are built, should be controlled effectively so as to develop a WMCB. Therefore, FLAC3D models were established to analyze the stability of the rock surrounding coal bunker #3 based on its geological conditions. Considering the symmetrical design of the coal bunker, the numerical model could be established as shown in Figure 11; the model size is 30 m × 15 m × 15 m. Furthermore, as can be seen from Figure 2(b) that the upper boundary of the bunker is the floor of the belt conveyor roadway, the distressed zone, which was free from the underground pressure, was set up at the top of the bunker in the numerical model (Figure 11). The rock parameters and constitutive model adopted in this model were same as those in the previous FLAC model.

The simulation results (Figure 12) indicate the following: (1) the surrounding rock in sandstone segments is basically stable, and the cumulative rock deformation is small (less than 25 mm); (2) the surrounding rock in coal seam segments, which moves into the inside of the bunker with a large deformation (80–110 mm) seen, is the main area of

Table 1: Physical and mechanical parameters of surrounding rock and concrete.

Strata	Density (kg·m^{-3})	Bulk modulus (GPa)	Shear modulus (GPa)	Friction angle (°)	Cohesion (MPa)
Coarse-grained sandstone	2600	5.0	4.0	28	2.0
Fine-grained sandstone	2500	4.0	3.0	26	1.7
Siltstone	2550	3.5	2.5	24	1.5
Coal seam #4-2	1400	1.3	0.9	18	0.3
Mudstone	1800	2.0	1.5	25	0.7
Clay	1500	2.0	1.3	23	0.4
Reinforced concrete	2700	5.0	4.0	32	2.2
Interface			$k_n = k_s = 125$ (GPa/m)		

Table 2: Mechanical parameters of floor strata after immersed in water for 36 h.

Strata	Elasticity modulus (MPa)	Bulk modulus (GPa)	Shear modulus (GPa)	Friction angle (°)	Cohesion (MPa)
Mudstone	1860	1.20	0.75	20	0.36
Clay	1650	1.30	0.64	18	0.22

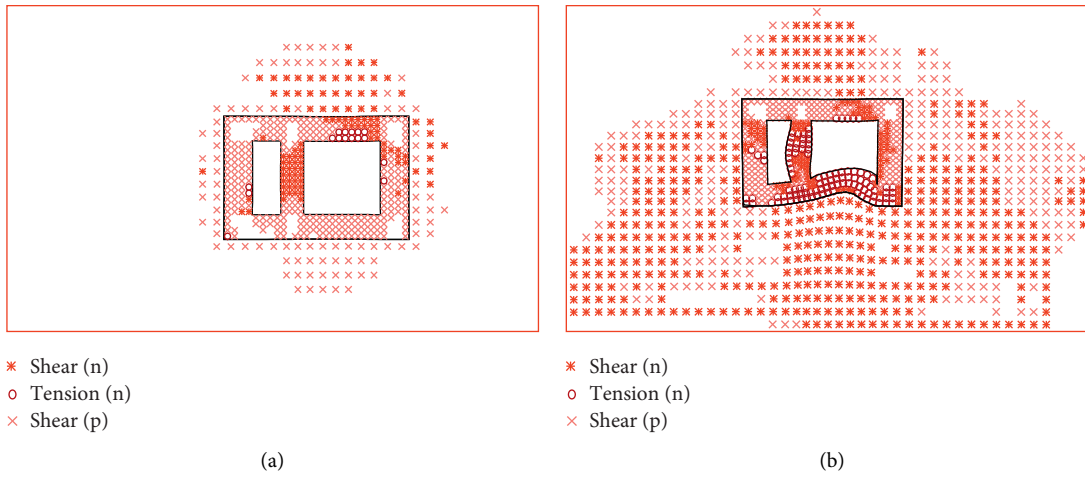

Figure 9: Comparison of plastic zone distribution under conditions (a) without water and (b) with water.

deformation in the entire surrounding rock mass; this is consistent with the results of field investigation.

To ensure the long-term stability of the surrounding rock and supporting structures, both the supporting strength and the supporting bearing system's stability should be taken into account. The bolt-cable combined supporting technology [8, 35] was adopted to control the deformation of the rock surrounding the coal bunker body. At the same time, significant attention should be paid to supporting the rock surrounding coal seam #4-2. Combined with research results of reinforcement mechanism of the bolting with the wire mesh system [36–38], specific reinforcement measures in this work were proposed as follows:

(1) The welded wire mesh, a more rigid screen, was used to increase the stiffness of supporting system for the coal seam segment

(2) The thickness of the support bearing structure formed by bolting, wire mesh, and shallow surrounding rock was increased by increasing the length of the bolt

(3) Apart from the high prestressed bolt and wire mesh system, compensation anchor cables were used to reinforce the support bearing structure formed by bolting, wire mesh, and shallow surrounding rock, which improved the stability of the supporting structure so as to control the deformation of the rock surrounding the coal seam segment, thus ensuring the stability of the overall rock mass around the bunker.

Based on the measures discussed above, six reinforcement schemes were designed, and a maximum displacement-monitoring point was set at the center of the coal seam segment (as shown in Figure 12) to evaluate their control effects. Additionally, the main parameters of the bolt and cable, which are both cable elements and available from the user's manual of FLAC3D, are listed in Table 3. It could be found from Table 4 that the maximum displacement of the coal seam segment decreases significantly from 89 mm to 36 mm when the length of the bolt increases from 2.4 m to 3.0 m and that of cable increases from 5.0 m to 6.2 m, respectively; however, the deformation then decreases to an insignificant extent when longer bolts and cables are used. Comparison of Schemes 5 and 6 shows that the reinforcing interval of the grouted anchor cables have a significant effect on the deformation. Therefore,

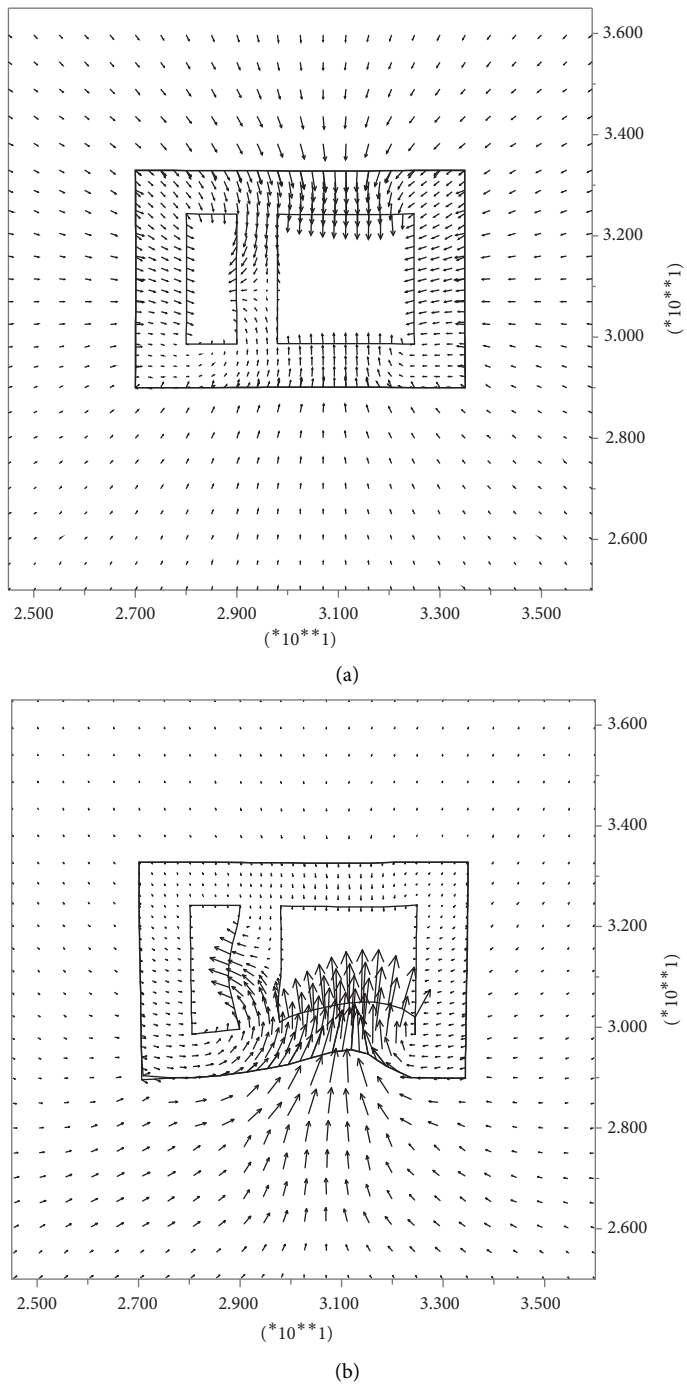

Figure 10: Comparison of displacement distribution under conditions (a) without water and (b) with water.

the reinforcing interval was selected as 1600 × 800 mm. Finally, an optimized scheme (Scheme 4) was determined (Figure 13) considering the cost, installation convenience, and technical feasibility. Figure 13 shows that

(1) The bolt and wire mesh were used to reinforce the shallow rock and coal mass at intervals of 800 mm × 800 mm, and the bolt nut's tightening pretension was not less than 60 kN.

(2) The bearing capacity of the deep surrounding rock was utilized by installation of the anchor cable (Φ17.8 mm × 6200 mm) with the spacing and row spacing being 1600 mm × 800 mm.

(3) The steel ladder bar and set with a diameter of Φ14 mm, along the inner surface of the bunker, were used to combine the bolts and anchors; thus, the overall stability of the supporting system was enhanced.

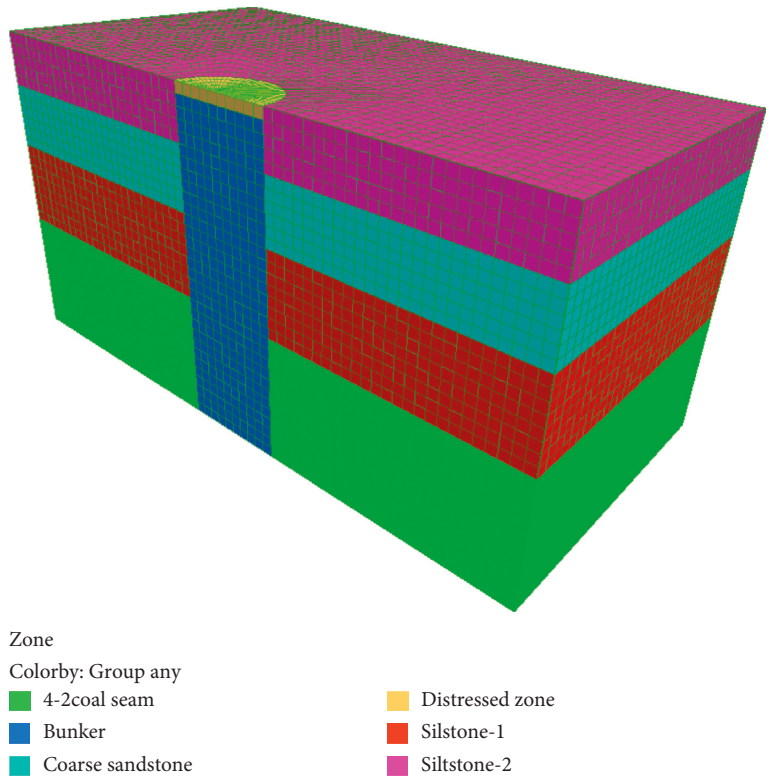

Figure 11: FLAC3D model of coal bunker #3.

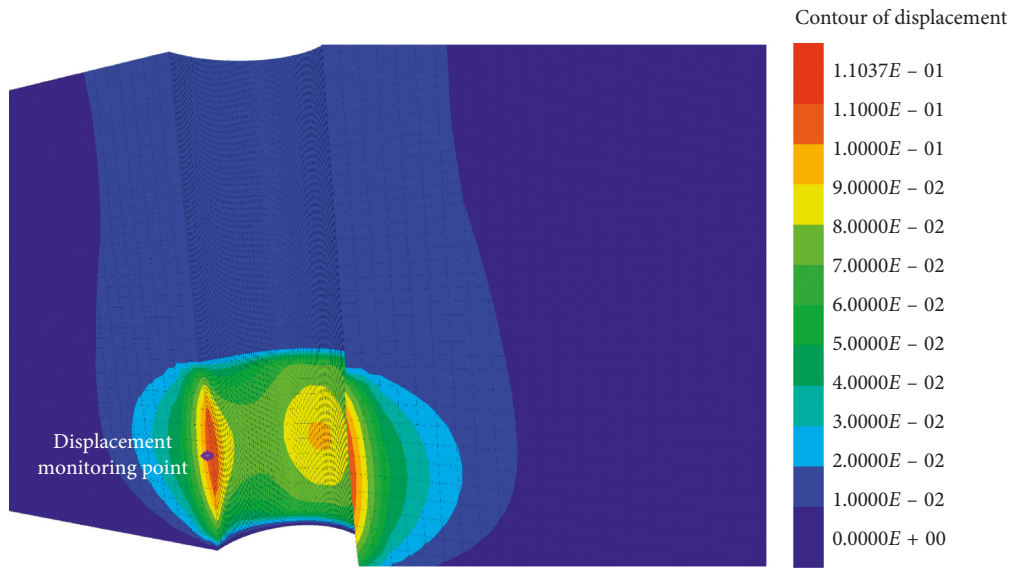

Figure 12: Deformation surrounding the body of coal bunker #3.

(4) Additionally, the Φ21.8 mm × 10,000 mm self-locking anchor cables (Figures 13–16), which will be explained in detail in a later section, are also used as compensation anchors and were reinforced to improve the stability of the supporting structure formed by the bolting and wire mesh in the coal seam segment. They also serve as the auxiliary carrying system, able to bear the full weight of the coal bunker, which ensured the long-term stability of the coal bunker.

3.2. Self-Bearing System of the Coal Bunker

3.2.1. Main Bearing System. As stated before, a new type of coal bunker, without the CFC, was invented to replace the traditional vertical coal bunker. The rock surrounding the bunker was controlled by a high-strength supporting scheme, described in a later section. Thus, the following section aims to solve two problems. The first is that a newly designed bearing system should be designed to bear the

Table 3: Parameters of the supporting elements used in the numerical model.

Property	Bolt	Cable
Dimensions (mm)	$Ø20 \times L_1$	$Ø17.8 \times L_2$
Elastic modulus (GPa)	25	200
Yield strength (kN)	150	450
Stiffness of the grout (N/m^2)	2×10^7	2×10^8
Cohesive capacity of the grout (N/m)	10×10^5	10×10^5
Grouted length (mm)	0.5 L_1	0.5 L_2
Pretension force (kN)	60	120

weight of coal stored in the bunker, concrete, bearing system itself, and feeder (as shown in Figure 2(b)); the second is that the hopper should be formed by a newly designed structure in the bearing system.

The specific design presented as follows: as the sandstone rock surrounding the upper part of the bunker is stable, the H-steel beams (Figures 2(b) and 14), installed in the sandstone rock uniformly and horizontally, bear the whole weight of coal bunker #3 without considering friction and adhesion between the concrete and the surrounding rock, so it was necessary to ensure that the carrying capacity of H-steel beams (Figures 14 and 15) was greater than the total weight of the coal bunker with a certain safety factor. Thus, this computation may be summarized as follows:

The bunker total weight is

$$M_T = M_{C1} + M_{C2} + M_B + M_F, \tag{2}$$

where M_{C1}, M_{C2}, M_B, and M_F are the weight of coal when the coal bunker is filled, the weight of concrete, the total weight of the H-steel brackets, and the weight of the feeder (Figure 2(b)), respectively. The weight borne by each H-steel beam is

$$M = \frac{M_T}{n}, \tag{3}$$

where n is the number of H-steel beams buried in the bunker wall rock. Then, the shear stress on the section of the H-steel beam is

$$\tau = \frac{Mg}{S}, \tag{4}$$

where S is the cross-sectional area of the H-steel beam.

Thus, the designed safety factor can be given by

$$K_1 = \frac{[\tau]}{\tau}, \tag{5}$$

where $[\tau]$ is the allowable shear stress in the H-steel beam.

As discussed above, the lower part of the surrounding rock is coal seam #4-2 with low strength which is unstable and could not be used to bear the weight of the hopper located in the bunker bottom (Figures 14 and 15). Then, to form the skeleton of the hopper and enhance the overall stability of the structure of the bunker, the H-steel brackets were designed and installed uniformly along the internal surface rock mass in the bunker (Figures 14 and 15). The upper ends of the H-steel brackets were embedded into the stable surrounding rock in the upper portion of the coal bunker; the bottom parts of brackets were fitted together to form the skeleton of the hopper. Additionally, the upper portions of H-steel brackets were fixed to the rock by the anchor cable, thus not only transferring the bearing capacity of the deep rock and improving the stability of the shallow surrounding rock, but also enhancing the stability of the frame formed by these H-steel brackets.

3.2.2. Assisted Bearing System. As the lower part of the bunker is the weak coal seam, there was a weak interface between the rock and coal seam (Figure 14). Furthermore, the bunker bottom was equipped with a hopper and a coal feeder, and the stability of the lower part of the bunker requires special attention. Then, the assisted bearing system, which included 16 self-locking anchor cables (Figure 16) arranged uniformly in the bunker funnel section along the bunker wall rock, was also designed to enhance the long-term stability of the whole bunker. Thus, the weight of the bunker hopper was borne by the sandstone and deep stable coal with the self-locking anchor cable anchored therein (the length of the anchor cables were 10,000 mm, ensuring that its anchoring ends were in the stable sandstone rocks), thereby ensuring the long-term stability of the coal bunker, which is beneficial to the stability of belt roadway under the coal bunker. Figure 16 shows the sample structure of the self-locking anchor cable. The vertical component force of the self-locking anchor cable is

$$F_v = nF \sin \alpha, \tag{6}$$

where n is the number of self-locking anchor cables, F_v is the vertical component force provided by the self-locking anchor cable, F is the single anchor bearing capacity, and α is the angle between the cable and the rock face, and given that the whole weight of the bunker is borne by the self-locking anchor cables, the designed safety factor can be given by

$$K_2 = \frac{F_v}{M_T g}. \tag{7}$$

3.2.3. Safety Assessment. The bunker body and hopper heights are 11,235 mm and 3,765 mm, respectively. According to the *Mining Engineering Design Manual* [39], the total thickness of concrete around the coal bunker is not less than 400 mm and the concrete strength is 40 MPa.

The total weight (concrete, coal, and coal-feeder beam) is calculated as follows:

$$\begin{aligned} V_1 &= \frac{1}{3}\pi H_1 \left[\left(\frac{D_1 + b_1}{2}\right)^2 - \frac{D_1 b_1}{4}\right], \\ Q &= V_1 + \frac{1}{4}\pi D_1^2 H_2, \\ V_2 &= \frac{1}{4}\pi D^2 H - Q, \\ M_{C1} &= \rho_{c1} Q, \\ M_{C2} &= \rho_{c2} V_2, \\ M_B &= P_l n_B L_B, \end{aligned} \tag{8}$$

Table 4: Six different reinforcement schemes and their control effect (unit: mm).

Scheme (no.)	Bolt (diameter × length)	Anchor cable (diameter × length)	Cable interval (spacing × row spacing)	Maximum displacement in coal seam segment
1	Φ20 × 2400	Φ17.8 × 5000	800 × 800	73
2	Φ20 × 2400	Φ17.8 × 5000	1600 × 800	89
3	Φ20 × 3000	Φ17.8 × 6200	800 × 800	36
4	Φ20 × 3000	Φ17.8 × 6200	1600 × 800	47
5	Φ20 × 3600	Φ17.8 × 7300	1600 × 800	32
6	Φ20 × 3600	Φ17.8 × 7300	1600 × 1600	61

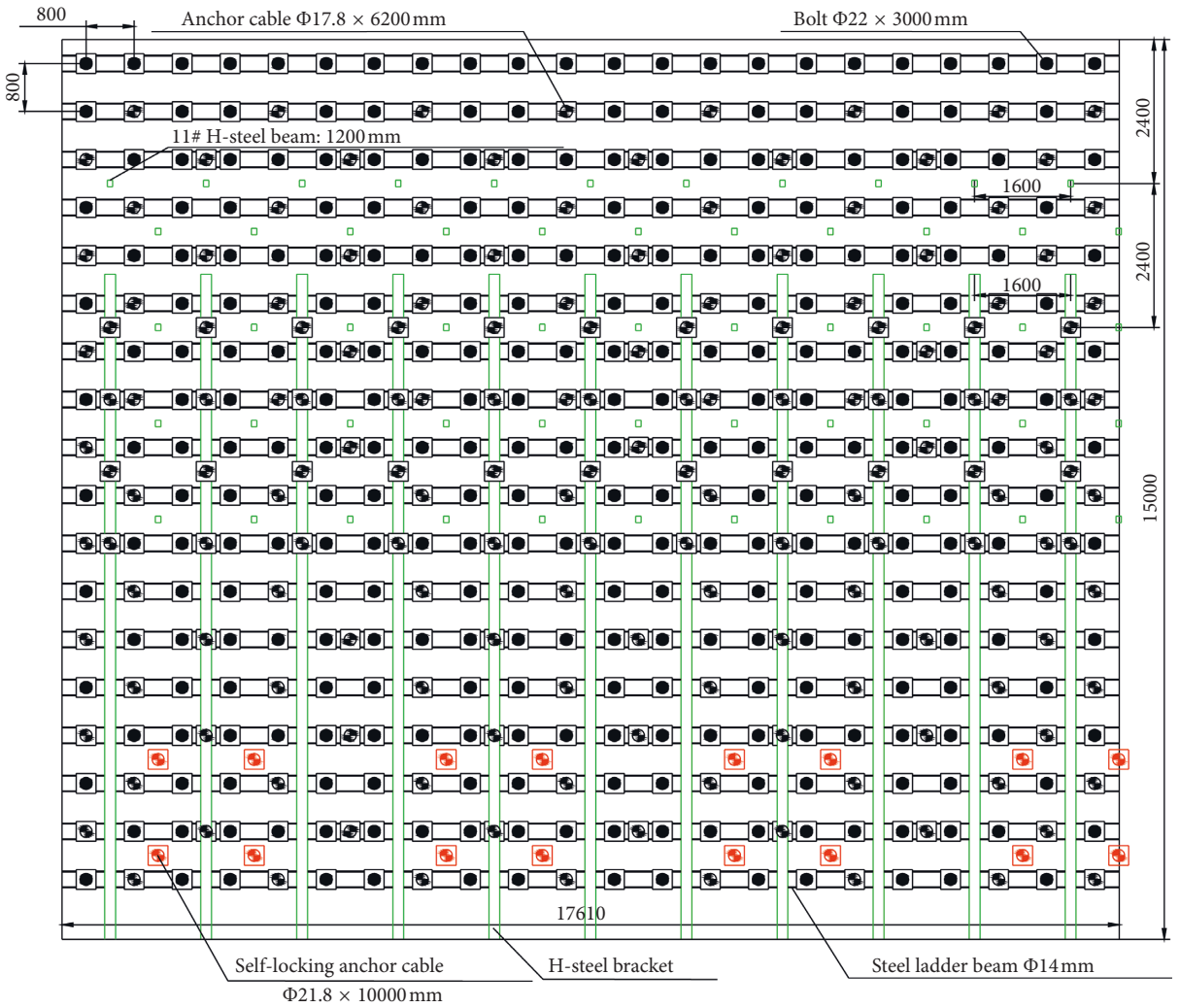

Figure 13: Expanded view of the supporting scheme for the coal bunker.

where V_1, Q, V_2, M_{c1}, M_{c2}, and M_B are the coal bunker's funnel volume, bunker volume, concrete volume, coal weight, concrete weight, and total weight of the H-steel brackets, respectively. H is the bunker design height, 15 m; H_1 is the coal funnel height, 3.765 m; H_2 is the bunker body height, 11.235 m; D is the section diameter of the bunker, 5.8 m; D_1 is the net cross-sectional diameter of the bunker, 5 m; b_1 is the mouth width of the funnel, 1.23 m; the weight of coal feeder is 4.5×10^3 kg; P_l is the lineal density of the H-steel, 26.05 kg/m; L_B is the H-steel bracket length, 15.013 m; n_B is the number of H-steel barn brackets, 12; and ρ_{c1} and ρ_{c2} are the density of the coal (1.4×10^3 kg/m^3) and concrete ($2.71.4 \times 10^3$ kg/m^3), respectively. These data are substituted into equation (2); thus, the value of M_T can be calculated to be 777.1×10^3 kg. With the number of H-steel beams being 60, its cross-sectional area being 0.003318 m^2, and its allowable shear stress being 125 MPa, the safety factor can be calculated as

$$K_1 = \frac{125}{38.25} = 3.26 > 3. \quad (9)$$

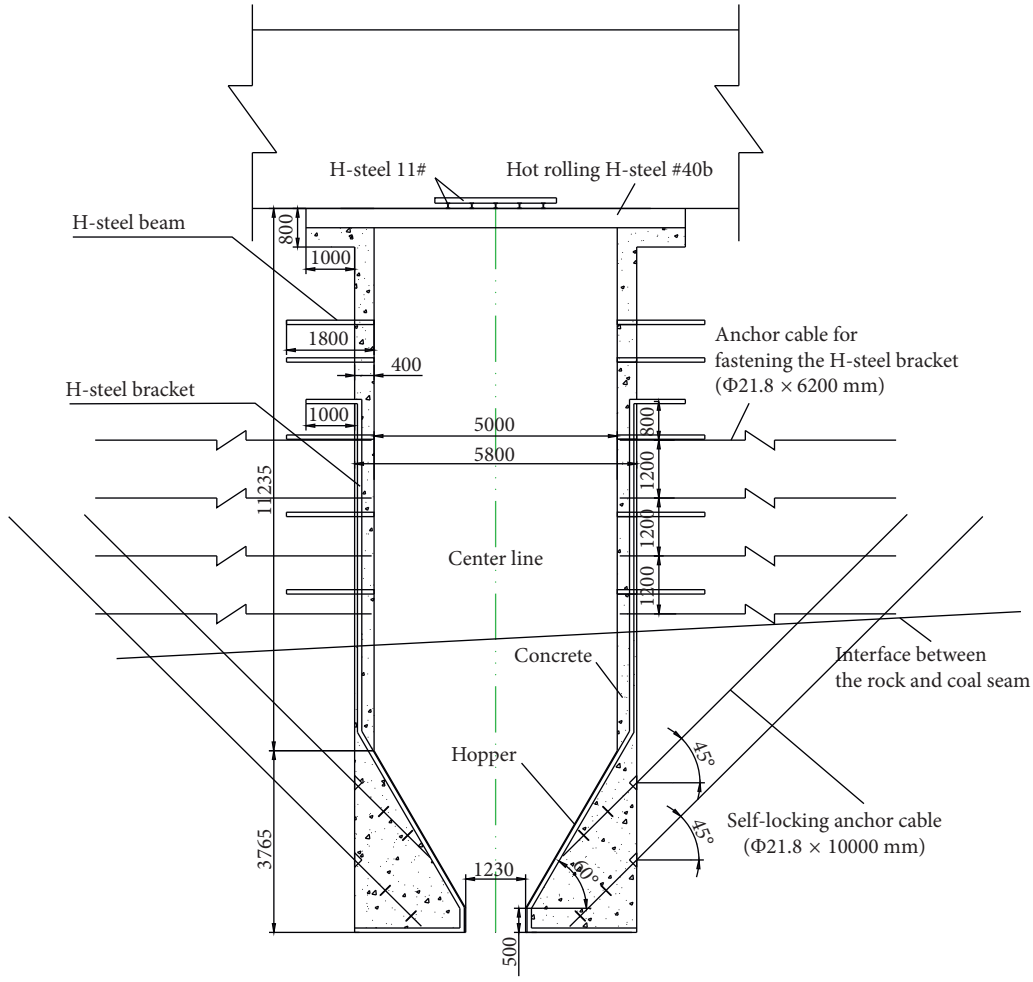

Figure 14: Schematic diagram of the WMCB.

Unlike surface buildings, for an underground rock engineering project, the long-term property of rocks in underground environment and the carry capacity loss of the supporting element should be considered. However, the related estimates are complex and difficult to quantify. According to the *Mining Engineering Design Manual* [39], the stability coefficient is designed to be 2.5, considering the factors such as variable loads, combined loads (including tension, bending, and torsion), ground pressure, and capacity loss of the bearing components; however, the long-term rock property of sandstone, which is the key bearing strata, should also be considered, so the long-term strength coefficient is set as 0.85. Thus, the rated safety factor in this bunker is assigned to be approximately 3. The calculated factor could meet safety requirements well. More importantly, the actual security needs to be verified by the following field engineering application.

The diameter of the self-locking anchor cable is 21.8 mm, and its carrying capacity is 458 kN. Substituting these data into equations (6) and (7), the designed safety factor can be calculated as follows:

$$K_2 = \frac{10361.792}{777.1 \times 9.8} = 1.36 > 1. \quad (10)$$

Here, because the assisted system serves to guarantee the long-term stability of the bunker, assume that all the weight of the bunker was carried by the assisted bearing system, the rated safety factor K_2 is assigned to be 1. Furthermore, certain safety reserves should be considered in underground buildings, so this meets safety requirements.

4. WMCB Application

In practice, the new bunker was built according to the following technical procedures (Figure 17). First, the roadway below the WMCB should be reinforced before the excavation of the WMCB by the anchor cables (Φ17.8 mm × 6200 mm) with the spacing and row spacing being 1600 mm × 800 mm, which was determined according to the specific reinforcement measures mentioned previously and acted as a compensating support. Second, excavate the circular coal bunker by means of stepwise deletion of the rocks, a total of 19 cycles with the excavating face advancing by 0.8 m from top to the bottom in every cycle, during which the bolt-mesh-cable system was installed immediately based on the supporting scheme (Figure 13). Third, install or fix the self-designed H-steel

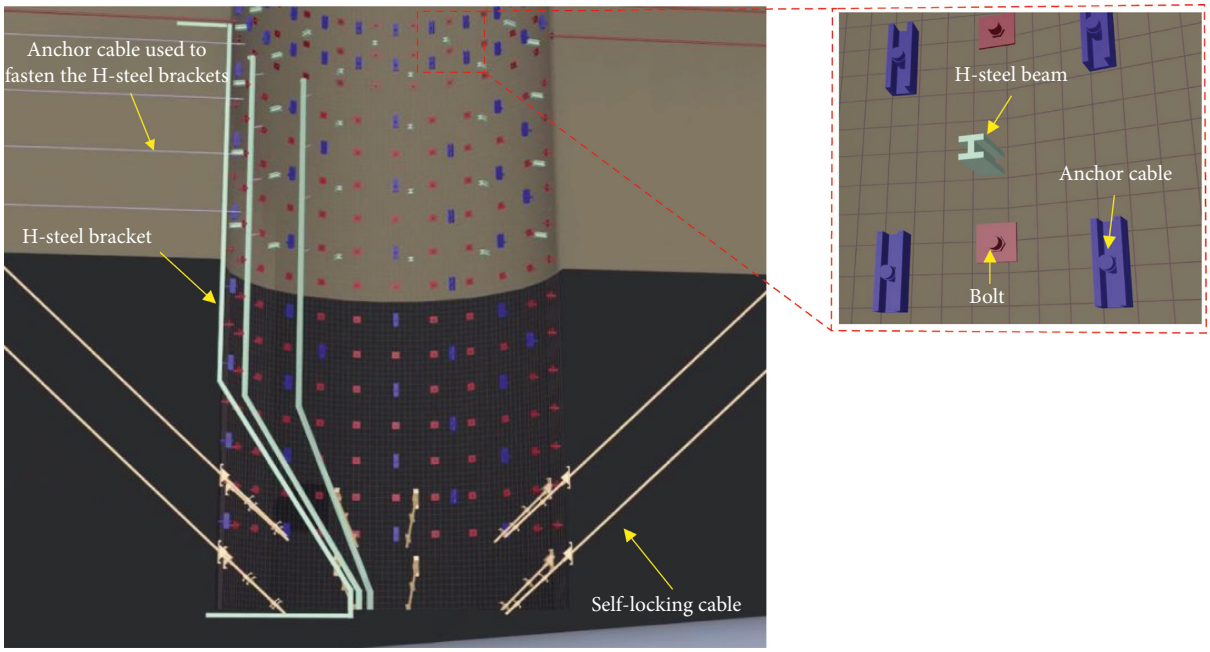

Figure 15: 3D view of the bearing structure of the WMCB.

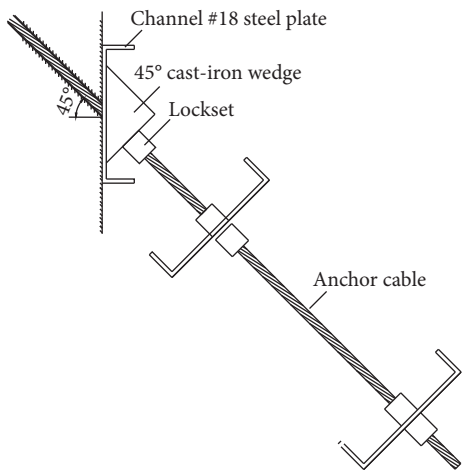

Figure 16: Structure diagram of the self-locking anchor cable.

beams, H-steel brackets, and the self-locking anchor cables based on the design scheme as shown in Figures 13 and 14. Fourth, configure rebars and carry out formwork around the bunker. Fifth, pour concrete into the space between the templates and the sidewall, thus immersing all the bearing elements in the concrete and forming the WMCB (Figures 2(b) and 15). Finally, complete the installation of related components at the top of the bunker, as shown in Figure 14.

The wall-mounted bunker had been in operation for five years (2013–2018). Long-term monitoring data (Figure 18) and site observation show that the cumulative slippage of the whole bunker body was 64.6 mm, the coal bunker diameter convergence measured by crossing method was 52.0 mm, and no cracking occurred at the reinforced concrete since the application of the WMCB.

The great economic benefits, due to the application of the WMCB, are shown in Table 5. As coal bunker #214 could remain stable less than three months after repair, it should be repaired for a month every time. The annual production capacity of the mine is 2.4 million tons, and the use of the WMCB gives rise to a production increase of more than two hundred thousand tons of coal every year (an economic benefit of 23.22 million USD at a unit-price of 38.69 USD per ton). Furthermore, the application of the WMCB reduces costs for the construction and maintenance of the original CFC; even though the construction cost of the WMCB is 0.582 million USD and the construction time is two months (production delay with a financial loss of 15.48 million USD), the coal mine has gained an economic benefit amounting to 101.906 million USD over five years.

5. Discussion

In this study, the influencing factors and failure mode of the CFC were revealed. Then, the WMCB was designed to avoid the influence of floor heave, during which, a self-bearing system, which included H-steel beams, H-steel brackets, and self-locking anchor cables, formed a replacement for the CFC to bear the whole weight of the bunker; thus, the whole weight was transferred to the stable and deep rocks. The stability of the new type of the coal bunker was verified in Xiashijie coal mine and made coal production therein more efficient.

Comparison of the WMCB and the traditional vertical coal bunker shows the differences between them, in that the former is a new vertical coal bunker without the CFC and can remain stable when the floor heave is severe or the strength of the floor rock is especially low; thus, the new coal bunker is a better solution to the floor heave issue. To date, no vertical coal bunkers without CFC have been reported. The new coal

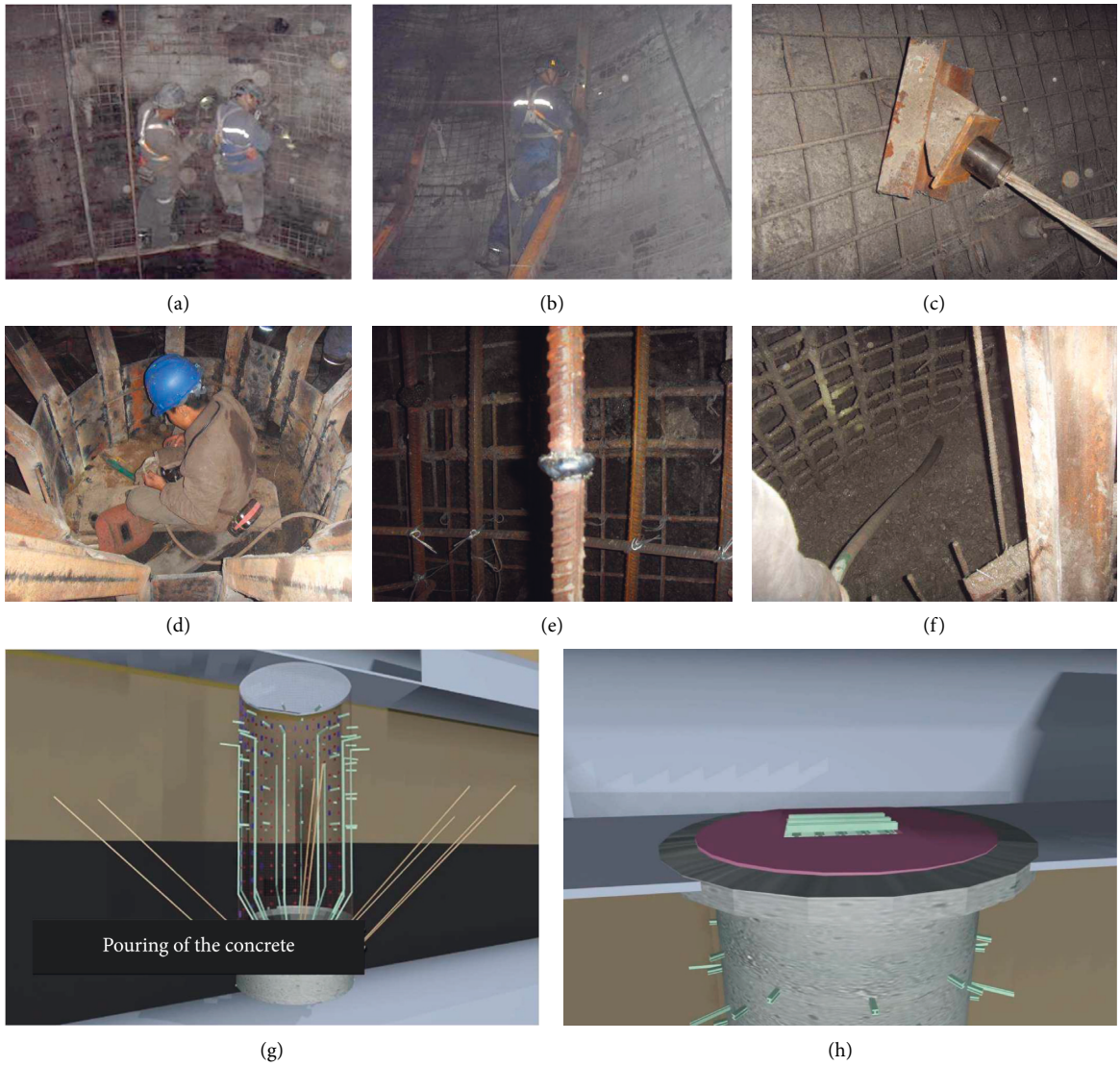

Figure 17: Construction procedures. (a) Installation of the bolt-mesh-cable system and the self-designed H-steel beams during stepwise excavation of the rocks, (b) installation of the self-designed H-steel brackets, (c) installation of the self-locking anchor cables, (d) fitting the bottom parts of H-steel brackets together to form the skeleton of the coal hopper, (e) configuring rebars around the bunker, (f) pouring concrete and (g) that was vibrated to remove any entrapped air bubbles, and (h) installation of related components at the top of the bunker.

bunker is stable and easy to maintain, and it offers great potential for application in mines with similar geological conditions. In addition, the newly designed coal bunker was granted a patent for invention in 2015 by State Intellectual Property Office of the People's Republic of China [40].

The work in this paper is preliminary, and the techniques used herein for stabilizing the coal bunker are mainly focused on field engineering. Further theoretical research should be performed in the future.

6. Conclusions

(1) The failure mechanism of the CFC was that the floor rocks were liable to swelling due to mine water. The strength of the floor rock decreased, and the swelling rock mass generated significant expansive forces. A much larger ranging plastic zone and deformation appeared in rocks surrounding the floor, causing tensile failure that occurred first in the floor concrete, further resulting in shearing damage in the sidewalls and tension and shearing collapse in the reinforced column, and eventually, overall instability of the CFC occurred.

(2) The WMCB was designed to replace the traditional vertical coal bunker, and the stability of its surrounding rock was simulated and analyzed. The results showed that the surrounding rock in the coal seam segment was the main deformation area. Then, the surrounding rock was controlled by an optimized high-strength bolt-cable support scheme. More importantly, a self-bearing system of the wall-mounted bunker was invented that was composed of

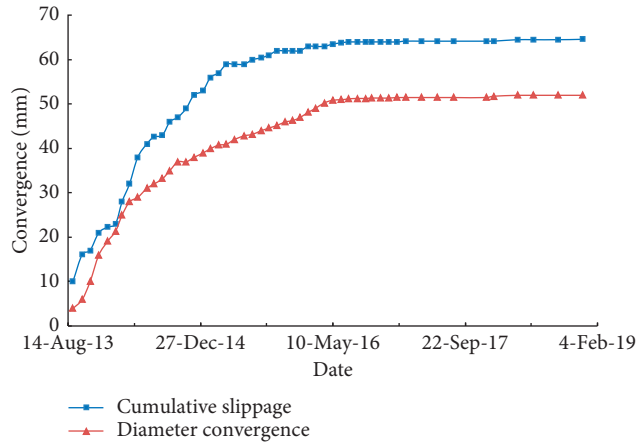

Figure 18: Monitoring of bunker fall and diameter convergence.

Table 5: Calculation of the economic benefits (unit: million UD).

Cost of coal bunker #214		Cost of repair of coal bunker #214 every year			Cost of the WMCB		
Construction cost	Construction time	Repair cost	Failure time	Delayed production efficiency	Construction cost	Construction time	Delayed production efficiency
$A = 0.398$	Two months	$B = 0.294$	Three months	$C = 23.22$	$D = 0.582$	Two months	$E = 15.48$
Net benefit over five years		$A + (B + C) \times 5 - D - E = 101.906$					

H-steel beams, H-steel brackets with fastened anchors, and self-locking anchor cables and was able to bear the whole weight of the coal bunker, thus negating the need for a bearing structure at the bottom.

(3) The WMCB differs from the traditional coal bunker in that the former, without the CFC, is easier to maintain than the latter, and it could be remain stable in spite of severe floor heave.

(4) The new coal bunker has been put into practice at Xiashijie coal mine, and its specific construction technology is presented in detail. Field testing proves that the WMCB, being stable and safe, contributes to a significant enhancement in production. The coal mine has accrued economic benefits amounting to 101.906 million USD over three years (2013–2018).

(5) It is key to construct a WMCB rather than a traditional coal bunker under geological conditions encompassing severe floor heave, loose (or fractured) and weak rock masses, and other similar conditions. The WMCB offers great prospects for application in other mines subject to similar geological conditions.

Data Availability

The data used to support the findings of this study are available from the corresponding author upon request.

Conflicts of Interest

The authors declare that there are no conflicts of interest regarding the publication of this paper.

Acknowledgments

We wish to thank Xiashijie coal mine for supporting this important study, as well as Xiaoquan Huo and Ming Xu for assistance with field construction and data collection. We would like to thank Editage (http://www.editage.cn) for English language editing. This work was funded by the State Key Laboratory of Coal Resources and Safe Mining, the China University of Mining and Technology (Grant No. SKLCRSM15X01), and the National Key Research and Development Plan (Grant No. 2017YFC0603001).

References

[1] L. M. Alotin and V. L. Belgorodskii, "Practice and theory of improving coal output by the use of a storage bunker in the transportation line," *Soviet Mineral Science*, vol. 6, no. 6, pp. 700–702, 1971.

[2] F. Liu, "Research on failure mechanism and its control technology of shaft coal pocket," Master's thesis, Chongqing University, Chongqing, China, 2008. in Chinese with English abstract.

[3] B. Sureshc, D. Carlos, and H. Michael, "Optimum bunker size and location in underground coal mine conveyor systems," *International Journal of Mining and Geo-Engineering*, vol. 5, no. 4, pp. 391–404, 1987.

[4] L. Wang, "Analysis and calculation of capacity of underground coal bunker," *Journal of Huainan Mining*, vol. 1, pp. 113–122, 1983.

[5] V. M. Shramko, "Influence of the collection bunker capacity to the utilization level of the main mine subsystems," *Soviet Mining Science*, vol. 20, no. 6, pp. 489–492, 1984.

[6] F. Duckmanton and R. Carlin, "Vertical bunker," *Colliery Guardian Redhill*, vol. 234, pp. 444–446, 1986.

[7] S. B. Tang and C. A. Tang, "Numerical studies on tunnel floor heave in swelling ground under humid conditions," *International Journal of Rock Mechanics and Mining Sciences*, vol. 55, pp. 139–150, 2012.

[8] Y. Kang, Q. Liu, G. Gong, and H. Wang, "Application of a combined support system to the weak floor reinforcement in deep underground coal mine," *International Journal of Rock Mechanics and Mining Sciences*, vol. 71, pp. 143–150, 2014.

[9] W. X. Zheng, Q. W. Bu, and Y. Q. Hu, "Plastic failure analysis of roadway floor surrounding rocks based on unified strength theory," *Advances in Civil Engineering*, vol. 2018, Article ID 9483538, 10 pages, 2018.

[10] W. Q. Peng, W. J. Wang, and C. Yuan, "Supporting technology research in deep well based on modified terzaghi formula," *Advances in Civil Engineering*, vol. 2018, Article ID 7475698, 6 pages, 2018.

[11] Q. A. Cui and J. J. Shen, "Location Selection of Coal Bunker Based on Particle Swarm Optimization," in *Proceedings of the 19th International Conference on Industrial Engineering*, pp. 1121–1128, Berlin, Heidelberg, Germany, June 2013.

[12] W. F. Ma, J. S. Chen, and J. C. Zhao, "Large-scale coal bunker engineering practice in deep shaft," *Shanxi Architecture*, vol. 38, pp. 117-118, 2012.

[13] H. T. Ma, "Design and construction technology of coal bunker with large diameter and high vertical height," *Coal Engineering*, vol. 47, pp. 42–44, 2015.

[14] Z. Q. Li, I. A. Oyediran, C. Tang, R. L. Hu, and Y. X. Zhou, "FEM application to loess slope excavation and support: case study of Dong Loutian coal bunker, Shuozhou, China," *Bulletin of Engineering Geology and the Environment*, vol. 73, no. 4, pp. 1013–1023, 2014.

[15] H. Wang, "Study on water inrush prevention technology of temporary coal bunker construction," *Coal Engineering*, vol. 16, pp. 46–48, 2013.

[16] H.-l. Lv, Y. Ma, S.-C. Zhou, and K. Liu, "Case study on the deterioration and collapse mechanism and curing technique of RC coal bunkers," *Procedia Earth and Planetary Science*, vol. 1, no. 1, pp. 606–611, 2009.

[17] R. Q. Dong, "Anti failure technology of 100 m high vertical coal silo," *Coal Science and Technology*, vol. 37, pp. 18–21, 2009.

[18] Q. Gong, "A study on coal bunker dredging technology under highly dynamic pressure and a portable dredger," *China Coal*, vol. 34, pp. 67–69, 2008.

[19] Q. Gong, "Analysis on blockage of coal bunker and its prevention," *Mining and Processing Equipment*, vol. 36, pp. 24–26, 2008.

[20] J. P. Sun and J. Jiang, "Laser monitoring of the coal level of coal silo by depth pre-calibration," *Journal of China Coal Society*, vol. 37, no. 1, pp. 172–176, 2012.

[21] Z.-A. Song, F. Zhan, C.-Y. Li, Z.-L. Wang, and S.-L. Zhang, "Research of the underground coal bunker clearing robot," *Journal of Coal Science and Engineering (China)*, vol. 16, no. 1, pp. 104–107, 2010.

[22] X. L. Zhao, J. W. Shen, and W. W. Shang, "Practice and research on natural ventilation of cylindrical coal bunker for gas exhaust," *Coal Engineering*, vol. 46, pp. 137–139, 2014.

[23] F. T. Wang, C. Zhang, S. F. Wei, X. G. Zhang, and S. H. Guo, "Whole section anchor-grouting reinforcement technology and its application in underground roadways with loose and fractured surrounding rock," *Tunnelling and Underground Space Technology*, vol. 51, pp. 133–143, 2016.

[24] GB/T 23561.14-2010, *Methods for Determining the Physical and Mechanical Properties of Coal and Rock—Part 14: Methods for Determining the Swelling Ratio of Rock*, State Standard of the People's Republic of China, Beijing, China, 2010.

[25] X. H. Wang, X. J. Du, G. R. Feng, and L. X. Kang, "The occurrence mechanism of rock burst in the three hard coal seam roadway," *Journal of Mining and Safety Engineering*, vol. 34, pp. 663–669, 2017.

[26] S. Liang, D. Elsworth, X. H. Li, X. H. Fu, B. Y. Sun, and Q. L. Yao, "Key strata characteristics controlling the integrity of deep wells in longwall mining areas," *International Journal of Coal Geology*, vol. 172, pp. 31–42, 2017.

[27] M. I. Álvarez-Fernández, C. González-Nicieza, A. E. Álvarez-Vigil, G. Herrera García, and S. Torno, "Numerical modelling and analysis of the influence of local variation in the thickness of a coal seam on surrounding stresses: application to a practical case," *International Journal of Coal Geology*, vol. 79, no. 4, pp. 157–166, 2009.

[28] X. J. Du, G. R. Feng, T. Y. Qi et al., "Roof stability analyses of water-preserved and water-stored coal mining with construction backfill mining," *Journal of China Coal Society*, vol. 44, pp. 820–829, 2019.

[29] T. Gentzis, N. Deisman, and R. J. Chalaturnyk, "A method to predict geomechanical properties and model well stability in horizontal boreholes," *International Journal of Coal Geology*, vol. 78, no. 2, pp. 149–160, 2009.

[30] D. Ma, X. Miao, H. Bai et al., "Effect of mining on shear sidewall groundwater inrush hazard caused by seepage instability of the penetrated karst collapse pillar," *Natural Hazards*, vol. 82, no. 1, pp. 73–93, 2016.

[31] E. Hoek and E. Brown, "Practical estimates of rock mass strength," *International Journal of Rock Mechanics and Mining Science & Geomechanics Abstracts*, vol. 34, no. 8, pp. 1165–1186, 1997.

[32] P. Marinos and E. Hoek, "GSI: a geologically friendly tool for rock mass strength estimation," in *Proceeding for the Geo. Eng. 2000 at the International Conference on Geotechnical and Geological Engineering*, pp. 1422–1446, Technomic Publishers, Melbourne, Australia, November 2000.

[33] Itasca Consulting Group, Inc., *Manual of FLAC Version 5*, Itasca Consulting Group, Inc., Minneapolis, MN, USA, 2005.

[34] C. Wu, J. Luo, R. J. Tian, G. Liu, H. K. Li, and X. L. Zhang, "The effect of Mud-shale hydration on rock mechanic parameters," *Journal of Oil, Gas Technology*, vol. 34, no. 4, pp. 147–150, 2012.

[35] Q. Meng, L. Han, J. Sun, F. Min, W. Feng, and X. Zhou, "Experimental study on the bolt-cable combined supporting technology for the extraction roadways in weakly cemented strata," *International Journal of Mining Science and Technology*, vol. 25, no. 1, pp. 113–119, 2015.

[36] B. Shen, "Coal mine roadway stability in soft rock: a case study," *Rock Mechanics and Rock Engineering*, vol. 47, no. 6, pp. 2225–2238, 2014.

[37] H. Basarir, Y. Sun, and G. Li, "Gateway stability analysis by global-local modeling approach," *International Journal of Rock Mechanics and Mining Sciences*, vol. 113, pp. 31–40, 2019.

[38] X. K. Wang, W. B. Xie, S. G. Jing, Z. L. Su, L. H. Li, and L. H. Lu, "Experimental study on large deformation control mechanism of surrounding rock of extremely loose coal roadway in gliding tectonics area," *Chinese Journal of Rock Mechanics and Engineering*, vol. 37, pp. 312–324, 2018.

[39] R. L. Zhang, G. W. He, and D. Li, *Mining Engineering Design Manual*, pp. 1550–1605, Coal Industry Press, Beijing, China, 2003.

[40] China University of Mining and Technology, *A Wall-Mounted Vertical Bunker Without A Coal Feeder Chamber*, State Intellectual Property Office of the People's Republic of China, Beijing, China, Grant No. CN201310465301.7, 2014.